total emitted intensities through identical slits in the parallel and perpendicular directions. Rotation of the field direction through 90° relative to the slits and photon counters would eliminate many systematic errors. Since R is independent of field strength in lowest order, nonuniformities in the field strength are not important, provided that the field direction remains well defined throughout the observation region. A small uncertainty δR in the measured value of R produces an uncertainty $\delta(\Delta E_L)$ in the Lamb shift given approximately by $\delta(\Delta E_L)/\Delta E_L \simeq \delta R/R$. It would also be of interest to verify that both the parallel and perpendicular intensity components decay with the same time constant.

ACKNOWLEDGMENTS

Financial support by the National Research Council of Canada is gratefully acknowledged. One of us (R. B. G.) is the holder of a NRC Bursary.

[1]G. W. Erickson, Phys. Rev. Lett. **27**, 780 (1971).
[2]C. Y. Fan, M. Garcia-Munoz, and S. A. Sellin, Phys. Rev. **161**, 6 (1967).
[3]M. Leventhal and D. E. Murnick, Phys. Rev. Lett. **25**, 1237 (1970).
[4]D. E. Murnick, M. Leventhal, and H. W. Kugel, Phys. Rev. Lett. **27**, 1625 (1971).
[5]H. W. Kugel, M. Leventhal, and D. E. Murnick, Phys. Rev. A **6**, 1306 (1972).
[6]W. E. Lamb, Jr. and R. C. Retherford, Phys. Rev. **79**, 549 (1950).
[7]H. K. Holt and S. A. Sellin, Phys. Rev. A **6**, 508 (1972).
[8]G. W. F. Drake, G. A. Victor, and A. Dalgarno, Phys. Rev. **180**, 25 (1969).
[9]W. R. Ott, W. E. Kauppila, and W. L. Fite, Phys. Rev. A **1**, 1089 (1970).
[10]G. W. F. Drake, Can. J. Phys. **50**, 1896 (1972).
[11]S. Klarsfeld, Phys. Lett. **30**, 382 (1969), and earlier references therein.
[12]C. Schwartz, Ann. Phys. (N.Y.) **6**, 156 (1959).
[13]C. Schwartz and T. J. Tieman, Ann. Phys. (N.Y.) **6**, 178 (1959).
[14]W. Zernik, Phys. Rev. **133**, 117 (1964).
[15]J. D. Garcia and J. E. Mack, J. Opt. Soc. Am. **55**, 654 (1965).
[16]J. S. Casalese and E. Gerjuoy, Phys. Rev. **180**, 327 (1969).

PHYSICAL REVIEW A VOLUME 8, NUMBER 1 JULY 1973

Calculation of Atomic and Molecular Momentum Expectation Values and Total Energies from Compton-Scattering Data

Irving R. Epstein
Department of Chemistry, Brandeis University, Waltham, Massachusetts 02154
(Received 8 February 1973)

Measurement of a system's Compton profile makes possible, in principle, the calculation of its electronic radial momentum distribution. From this quantity, the expectation values $\langle p^n \rangle$ and the total energy may be obtained. The feasibility of using Compton-scattering data in this way is examined in view of the limitations imposed by (i) random experimental errors on the measured profile, and (ii) restriction of the profile data to a finite range of momenta. It is concluded that while present techniques may be adequate for a few systems, improved experimental methods are required before Compton scattering becomes a useful source of atomic and molecular energies.

I. INTRODUCTION

Recent years have seen a tremendous revival of interest in Compton scattering as a tool for studying electronic momentum distributions in atoms, molecules, and solids.[1] Significant experimental advances have occured in both x-ray[2,3] and γ-ray[4,5] techniques. Compton profiles over a broad range of momenta and accurate to a fraction of a percent at the peak may now be obtained in a matter of days, even for relatively heavy elements.[5]

Compton-scattering measurements yield, at least in principle, a full one-dimensional (or, in the case of anisotropic systems, three-dimensional) momentum distribution for the scatterer. It should therefore be possible to calculate from Compton data expectation values of operators which are functions of momentum. In particular, one should be able to obtain the quantities

$$\langle p^n \rangle = \int_0^\infty p^n I(p)\, dp, \tag{1}$$

where $I(p)$ is the (normalized) radial momentum distribution function. The value $n = 2$ in Eq. (1) is of special interest, since $\frac{1}{2}\langle p^2\rangle$ gives the electronic kinetic energy and, by application of the virial theorem, the total energy of the scattering system.

The possibility of obtaining atomic and molecular total energies would seem to make Compton scattering an extremely attractive technique, particularly since these energies are generally derived from spectroscopic and/or thermodynamic quantities which are often difficult or impossible to measure to high accuracy. In view of both the crucial role played by the variational principle in molecular quantum mechanics and the many recent efforts to calculate correlation energies,[6] it would be extremely desirable to have another experimental source of atomic and molecular energy values.

To our knowledge, the literature contains no calculations of total energies or momentum expectation values other than $\langle p^{-1}\rangle$ from experimental Compton-scattering data. There exist at least three major obstacles to the accurate measurement of $\langle p^2\rangle$ and related quantities by Compton scattering.

First, the momentum distribution which appears in Eq. (1) is not measured directly. One measures the Compton profile $J(q)$ and then obtains $I(p)$ by numerical differentiation of the profile. The relationship between $J(q)$ and $I(p)$ is well defined and many workers[7] have used their results to obtain radial momentum distributions. However, numerical differentiation of experimental data is an undesirable procedure, because it tends to magnify the errors in the data points. A quantitative consideration of this problem in Compton scattering has been given by Cheng, Williams, and Cooper.[8] In Sec. II we show how the numerical differentiation procedure usually used to obtain $I(p)$ may be replaced by an integration which yields $\langle p^n\rangle$ directly, thereby minimizing the introduction of numerical inaccuracies.

A second difficulty is that the measured Compton profile, and hence the momentum distribution, is obtained over a limited set of momenta. One can measure the Compton-scattered intensity only over a finite range of wavelengths. The effects of this truncation of the momentum distribution on the calculation of expectation values are considered in Sec. III.

Even if one could measure Compton profiles over an arbitrarily large range of momenta and even if one could eliminate errors from numerical procedures, one would still be left with the statistical and other errors on the individual data points. In Sec. IV an attempt is made to assess the effects of experimental error on the calculation of $\langle p^n\rangle$.

In Sec. V, we consider the implications of the problems discussed above. We suggest some ways in which experimental conditions might be selected to facilitate the measurement of the quantities $\langle p^n\rangle$ and we look at the feasibility of obtaining accurate values with present techniques.

II. GENERAL THEORY

Most Compton-scattering studies employ the impulse approximation (IA) to relate the Compton profile and the radial momentum distribution. In the IA one assumes that the time of interaction between the photon and the electron is sufficiently short that the electron's potential energy remains essentially unchanged during the interaction. An alternative statement of the IA is that the binding energy of the electron is negligible with respect to the energy transferred to it by the photon. If the IA holds, then the relationship of the Compton profile $J(p_z)$ along a particular direction of scattering to the three-dimensional momentum distribution $I(p_x, p_y, p_z)$ is given by[9,10]

$$J(p_z) = \int_{p_x}\int_{p_y} I(p_x, p_y, p_z)\, dp_x\, dp_y . \tag{2}$$

For an isotropic system, (2) reduces to

$$J(q) = \tfrac{1}{2}\int_{|q|}^{\infty} [I(p)/p]\, dp, \tag{3}$$

where

$$I(p) \equiv 4\pi \int p^2 I(\vec{p})\, d\Omega_p .$$

The intensity of Compton-scattered radiation at "reduced wavelength" q is proportional to $J(q)$. The observed wavelength λ of the scattered photons is given by

$$q = mc\,\frac{\lambda - \lambda_0 - (2h/mc)\sin^2\frac{1}{2}\varphi}{2\lambda_0 \sin\frac{1}{2}\varphi},$$

where λ_0 is the incident photon wavelength, φ is the angle of scattering, and $2h/mc$ is the Compton wavelength. Equation (3) is easily inverted to yield

$$I(p) = -2p\,\frac{dJ(p)}{dp} \qquad (p>0). \tag{4}$$

Eisenberger and Platzmann[11] have analyzed the accuracy of the impulse approximation and have obtained exact non-IA Compton profiles for electrons in hydrogenlike 1s orbitals. Currat *et al.*[12] have calculated numerical non-IA profiles for 2s and 2p electrons. It does not appear possible, however, to invert these results to obtain momentum distributions from measured profiles. Thus we are left with Eq. (4). Fortunately, the situation is far from bleak. In reviewing the validity

of the IA, Cooper concludes that even for x-ray experiments "the simple interpretative procedure of the impulse approximation is valid for (the vast majority of) experiments of the accuracy at present attained."[1a] The recent development of γ-ray Compton scattering makes it likely that future experiments will be performed at photon energies which make the IA nearly exact.[5]

Let us assume, then, that we may work within the framework of the IA. Combining Eqs. (1) and (4), we have

$$\langle p^n \rangle = -\int_0^\infty 2p^{n+1} \frac{dJ(p)\,dp}{dp} .$$

Integration by parts gives

$$\langle p^n \rangle = -2p^{n+1} J(p)\Big|_0^\infty + 2(n+1)\int_0^\infty p^n J(p)\,dp . \quad (5)$$

In order for the integral to converge, $J(p)$ must go to zero as $p \to \infty$ faster than $p^{-(n+1)}$. If this is the case, then the first term in Eq. (5) vanishes for all non-negative n, and we have simply

$$\langle p^n \rangle = 2(n+1)\int_0^\infty p^n J(p)\,dp \quad (n>0). \quad (6)$$

Equation (6) enables us to calculate $\langle p^n \rangle$ directly from the experimental data without the intermediate step of numerical differentiation via Eq. (4). It also facilitates analysis of the various contributions to the error in $\langle p^n \rangle$, as we shall see in the following sections.

III. EFFECTS OF TRUNCATION OF MOMENTUM RANGE

There are a number of factors which determine the range of momenta over which a Compton profile is to be measured. In x-ray experiments one is limited by the small signal-to-noise values obtainable at high q, by difficulties in determining a background of questionable linearity, and by the overlap of peaks from other orders of reflection and from other x-ray lines. In γ-ray Compton scattering there is a single, relatively narrow line and a much lower, easier-to-measure background. No problems arise from other orders of reflection, since one uses a solid-state detector and multichannel analyzer in place of the analyzing crystal. The limiting factors in a γ-ray experiment are thus the energy range of the detector, the number of channels available, and the design of the experiment, i.e., the choice of whether to measure the profile at closely spaced points over a shorter range or to take more widely spaced readings over a broader range. γ-ray meausrements of $J(q)$ for krypton over a range of 30 a.u. have recently been reported.[5]

In practice, most experiments appear to be designed to provide the smallest interval between profile points consistent with the requirement that there be sufficient high-momentum data to give the correct normalization integral $\langle p^0 \rangle$. The question that we ask here is whether such experiments can be expected to yield reliable values for $\langle p^2 \rangle$ and for other quantities of interest. Aside from the total energy, the other observable directly available from the Compton profile is $\langle p^{-1} \rangle$ which, from Eq. (3), is seen to be equal to half the peak height of the profile, $\frac{1}{2}J(0)$. It may prove possible to correlate $\langle p \rangle$, the average magnitude of the current density, with some molecular property such as the nuclear magnetic resonance spectrum, but such a relationship remains to be developed. Relativistic energy corrections are proportional to $\langle p^4 \rangle$.

It is clear that the accuracy of $\langle p^{-1} \rangle$ depends only upon the normalization of the profile and hence only upon the condition that $\langle p^0 \rangle = 1$ per electron. However, $\langle p \rangle$, $\langle p^2 \rangle$, and higher powers of the momentum operator weight the high-momentum region of the distribution more heavily and may be poorly described by data sufficient to give accurate normalization. We now undertake a calculation to assess the accuracy attainable for the quantity $\langle p^n \rangle$ as a function of the highest momentum at which the Compton profile is measured, p_h.

Consider the quantity

$$(p^n)_h = -2p_h^{n+1} J(p_h) + 2(n+1)\int_0^{p_h} p^n J(p)\,dp \quad (n \geq 0). \quad (7)$$

Since $J(p)$ is a non-negative function of p, it is clear from Eqs. (5) and (6) that $(p^n)_h$ represents the contribution to $\langle p^n \rangle$ from that part of the momentum distribution with $p \leq p_h$, and that

$$(p^n)_h \leq 2(n+1)\int_0^{p_h} p^n J(p)\,dp \leq 2(n+1)\int_0^\infty p^n J(p)\,dp = \langle p^n \rangle .$$

That is, given the Compton profile over a momentum range from 0 to p_h, the integral on the right-hand side of Eq. (7) represents a *better* estimate of $\langle p^n \rangle$ than does the integral in Eq. (1) over the same range of integration. We therefore define the nth *partial expectation value* $p^n(p_h)$ as

$$p^n(p_h) = 2(n+1)\int_0^{p_h} p^n J(p)\,dp \quad (n \geq 0). \quad (8)$$

We note that $p^n(p_h)$ increases monotonically, and that

$$\lim p^n(p_h) = \langle p^n \rangle \quad \text{as } p_h \to \infty .$$

For wave functions composed of Slater- or Gaussian-type atomic orbitals (STOs or GTOs) one may calculate the quantities $I(p)$, $J(p)$, and $p^n(p_h)$ analytically.[13] Since atoms and molecules may be described in terms of minimal basis sets

TABLE I. Properties of $1s$ and $2p$ STOs with orbital exponent a.

	$1s$	$2p$ [a]
$\psi(r)$	$(a^3/\pi)^{1/2}e^{-ar}$	$(a^5/3\pi)^{1/2}re^{-ar}Y_{1m}(\theta,\varphi)$
$\chi(p)$	$(8a^5/\pi^2)^{1/2}(a^2+p^2)^{-2}$	$(128a^7/3\pi^2)^{1/2}i^{-1}p(a^2+p^2)^{-3}Y_{1m}(\theta_p,\varphi_p)$
$I(p)$	$(32a^5/\pi)p^2(a^2+p^2)^{-4}$	$(512a^7/3\pi)p^4(a^2+p^2)^{-6}$
$J(p)$	$(8a^5/3\pi)(a^2+p^2)^{-3}$	$(32a^7/15\pi)(a^2+5p^2)(a^2+p^2)^{-5}$

[a] The functions $Y_{1m}(\theta,\varphi)$ are normalized so that $\int d\Omega Y^*_{1m}(\theta,\varphi)Y_{1m'}(\theta,\varphi)=4\pi\delta_{mm'}$.

of STOs with well-characterized orbital exponents, we shall confine our discussion here to the STO case.[14] Computations with GTOs are somewhat simpler, but questions involving the number of orbitals and choice of orbital exponents necessary to describe a particular system make GTOs less desirable for application to the question at hand.

We investigate the behavior of $p^n(p_h)$ for $1s$ and $2p$ STOs. The relevant properties of such orbitals are shown in Table I. The orbitals are first converted from the position to the momentum representation $\psi(\vec{x})\rightarrow\chi(\vec{p})$ by a Fourier transform. The quantities $I(p)$ are then obtained by squaring the momentum wave function and integrating over the momentum space angular variables. Equation (3) yields the Compton profile $J(p)$, which is then inserted into Eq. (8). Since for large p, $J(p)\sim p^{-(2l+6)}$, where l is the angular quantum number, the integral in Eq. (8) converges only for $n\leq 2l+4$. Thus for s orbitals, we are limited to the range $0\leq n\leq 4$. On performing the calculation, we find that all the quantities $p^n(p_h)$ have the form

$$p^n(p_h)=a^n p^n(p_h/a), \tag{9}$$

where a is the orbital exponent.[15] We may therefore express the partial expectation values in terms of the dimensionless parameter $s=p_h/a$. The orbital exponent a simply acts as a scaling factor.

Exact expressions for the $p^n(s)$, $0\leq n\leq 4$, are given in Table II for $1s$ and $2p$ STOs. A more convenient quantity for determing the desired range of momenta for a particular experiment is the relative truncation error in $\langle p^n\rangle$, defined by

$$\Delta^n(s)=1-p^n(s)/\langle p^n\rangle . \tag{10}$$

The behavior of $\Delta^n(s)$ is shown in Figs. 1 and 2 for $1s$ and $2p$ STOs, respectively. Suppose that one wished to measure $\langle p^3\rangle$ for H_2 to 1% accuracy by Compton scattering. The condition to be met is that $\Delta^3(s)$ be less than or equal to 0.01. The hydrogen molecule is well described by $1s$ STOs with exponent ~ 1.2. From Fig. 1, $\Delta^3(s)=0.01$ for $s\approx 14.2$. Thus one should be able to obtain 1% accuracy in $\langle p^3\rangle$ for $p_h\geq 14.2(1.2)=17.0$ a.u.

Several qualitative features emerge from Figs. 1 and 2. First, highly accurate values (better than 1%) will be exceedingly difficult to obtain, particularly for $1s$ orbitals of heavier elements (for $1s$ orbitals a is slightly less than the atomic number). The situation appears more fortuitous for $2p$, and also for $2s$, $3d$, and other orbitals, not only because the $\Delta^n(s)$ curves reach small values at lower momentum, but also because the orbital exponents are smaller for orbitals of higher principle quantum number.[15]

One might expect the slow convergence of $\langle p^n\rangle$ for $1s$ orbitals to be somewhat less important for heavier elements, since the $1s$ electrons would constitute a smaller fraction of the atom. However, it must be borne in mind that $\langle p^n\rangle$ varies as a^n or, for $1s$ orbitals, roughly as the nth power of the atomic number. Thus even for argon ($Z=18$), the two $1s$ electrons contribute

TABLE II. Partial expectation values $p^n(s)$ for STOs with orbital exponent a.

n	$1s$	$2p$
0	$(2/3\pi)[(3s^2+5s)(1+s^2)^{-2}+3\tan^{-1}s]$	$(1/15\pi)[(30s^7+110s^5+146s^3+34s)(1+s^2)^{-4}+30\tan^{-1}s]$
1	$(8a/3\pi)[1-(1+s^2)^{-2}]$	$(64a/45\pi)[2-(5s^2+2)(1+s^2)^{-4}]$
2	$(2a^2/\pi)[(s^2-s)(1+s^2)^{-2}+\tan^{-1}s]$	$(a^2/15\pi)[(30s^7+110s^4-46s^3-30s)(1+s^2)^{-4}+30\tan^{-1}s]$
3	$(16a^3/3\pi)[s^4(1+s^2)^{-2}]$	$(64a^3/15\pi)[1-(5s^4+4s^2+1)(1+s^2)^{-4}]$
4	$(10a^4/3\pi)[-(5s^3+3s)(1+s^2)^{-2}+3\tan^{-1}s]$	$(128a^4/9\pi)[(21s^7-83s^5-77s^3-21s)(1+s^2)^{-4}+\frac{21}{64}\tan^{-1}s]$

about 59% of the total $\langle p^2 \rangle$. For values of n greater than 1, we expect then that $\langle p^n \rangle$ will be most readily measurable for the lightest elements.

Our analysis has been carried out in terms of one-parameter atomic orbitals. Nevertheless, the success of wave functions composed of linear combinations of such orbitals in describing a wide range of molecular properties suggests that the results obtained here should provide reasonable estimates of the relative truncation errors and hence of the momentum range required for a given accuracy in $\langle p^n \rangle$ for any system of interest.

IV. EFFECTS OF EXPERIMENTAL ERROR

Suppose that a Compton profile has been measured over a momentum range sufficiently large that the truncation error is negligible. There still remains the problem that no data point is measured exactly. Each point has associated with it a random and possibly a systematic error. The question is what effect the errors on individual profile points will have on the value of $\langle p^n \rangle$ calculated by the methods described above.

From Eq. (8), we see that an error $\epsilon(q)$ in the profile $J(q)$ will give rise to an error in $p^n(p_h)$ of the form

$$e_n = 2(n+1)\int_0^{p_h} q^n \epsilon(q)\, dq. \tag{11}$$

Which expectation value will be most affected will, of course, depend on the exact form of $\epsilon(q)$. In principle, one should be able to use Eq. (11) in conjunction with calculated values of $\langle p^n \rangle$ to search for systematic errors in the data.

The problem of random, statistical errors requires a somewhat more detailed analysis. Consider a Compton profile $J(q)$ measured at points $0 = q_0, q_1, \ldots, q_m = p_h$ and suppose that c_j counts are collected at q_j. Then the variance of the random variable $J(q_j)$ is given by

$$\sigma_j^2 = J_j^2 / c_j, \tag{12}$$

where J_j is the exact value of the Compton profile at q_j. If we define quantities

$$G_j = J(q_j) - J_j \quad (j = 0, 1, \ldots, m), \tag{13}$$

then G_j is a normally distributed random variable with mean zero and variance σ_j^2. Since G_j are independent, the $(m+1)$-dimensional vector which they form constitutes an $(m+1)$-variate normal distribution with probability density function

$$\varphi(\underline{G}) = C \exp(-\tfrac{1}{2}\underline{G}^T \bar{M}_g^{-1} \underline{G}), \tag{14}$$

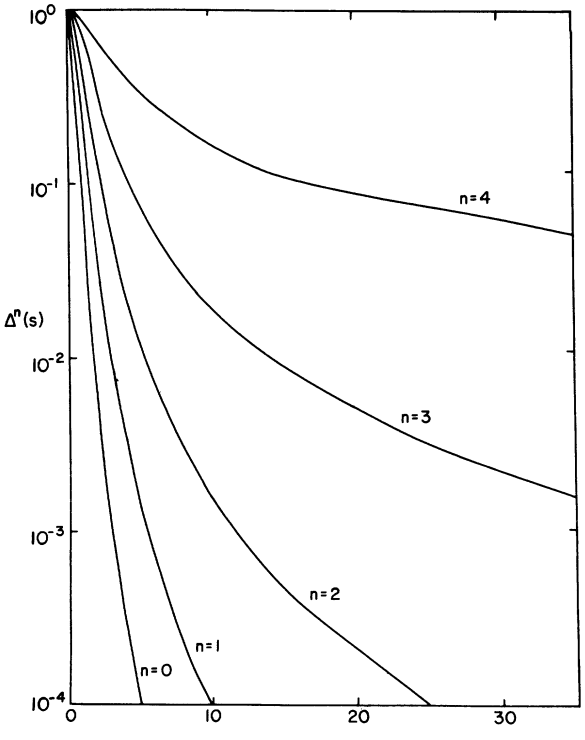

FIG. 1. Relative truncation error $\Delta^n(s)$ in $\langle p^n \rangle$ for Slater-type 1s orbitals ($s = p_h/a$, where a is the orbital exponent).

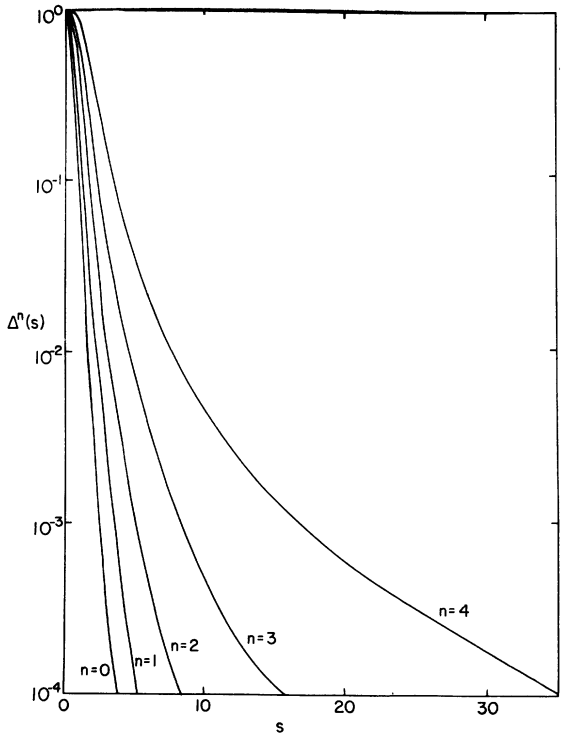

FIG. 2. Relative truncation error $\Delta^n(s)$ in $\langle p^n \rangle$ for Slater-type 2p orbitals.

where C is a normalization constant, $\underline{G}^T$ denotes the transpose of $\underline{G}$, and $\vec{\vec{M}}_g$ is the variance-covariance matrix of the distribution. In this case

$$(\vec{\vec{M}}_g)_{ij} = \sigma_j^2 \delta_{ij}, \tag{15}$$

with σ_j given by Eq. (12).[16]

What we seek is the form of the distribution for the vector $\vec{F}$ defined by

$$F_i = \langle p^i \rangle - \langle p^i \rangle_{\text{exact}}, \tag{16}$$

where the first expectation value is that obtained from the experimental $J(q_j)$ via numerical integration of Eq. (8) and the "exact" value is calculated in the same way but with the true values J_j. To obtain the probability density function for $\vec{F}$, we make use of the following result.[17]

If two vectors of random variables, $\vec{F}$ and $\vec{G}$, each have zero mean and are linearly related such that

$$\vec{F} = \vec{\vec{T}} \cdot \vec{G} \tag{17}$$

and if the variance-covariance matrix of $\vec{G}$ is $\vec{\vec{M}}_g$, then the variance-covariance matrix of $\vec{F}$ is given by

$$\vec{\vec{M}}_f = \vec{\vec{T}} \cdot \vec{\vec{M}}_g \cdot \vec{\vec{T}}^T. \tag{18}$$

In the special case where $\vec{G}$ is normally distributed with a density function of the form shown in Eq. (15), $\vec{F}$ is normally distributed with density function

$$\varphi(\vec{F}) = C' \exp(-\tfrac{1}{2} \vec{F}^T \cdot \vec{\vec{M}}_f^{-1} \cdot \vec{F}), \tag{19}$$

where C' is a normalization conatant and $\vec{\vec{M}}_f$ is obtained from $\vec{\vec{M}}_g$ by use of Eq. (18).

Suppose that the numerical integration scheme employed to obtain $\langle p^n \rangle$ from Eq. (8) is defined by a set of weights w_j, $j = 0, 1, \cdots, m$. That is,

$$\int_0^{q_m} f(q)\, dq = \sum_{j=0}^{m} w_j f(q_j). \tag{20}$$

Combining Eqs. (8), (13), (16), and (20), we may write

$$F_i = 2(i+1) \sum_{j=0}^{m} w_j q_j^i [J(q_j) - J_j] = 2(i+1) \sum_{j=0}^{m} w_j q_j^i G_j. \tag{21}$$

Thus the matrix $\vec{\vec{T}}$ in Eq. (17) is defined by

$$\vec{\vec{T}}_{ij} = 2(i+1)\, w_j q_j^i, \tag{22}$$

where the w_j specify a particular integration scheme according to Eq. (20). Inserting Eqs. (15) and (22) into Eq. (18), we find that

$$(M_f)_{ij} = 4(i+1)(j+1) \sum_{k=0}^{m} w_k^2 q_k^i q_k^j \sigma_k^2,$$

and hence the variance in $\langle p^i \rangle$ is just[18]

$$s_i^2 \equiv (M_f)_{ii} = 4(i+1)^2 \sum_{k=0}^{m} w_k^2 q_k^{2i} \sigma_k^2. \tag{23}$$

In most Compton-scattering experiments, the data points are equally spaced, so that $q_k = k\Delta$, where Δ is the spacing between profile points. If one assumes for the sake of computational convenience that all the points have the same variance σ_0^2 (i.e., $c_i = J_0^2/\sigma_0^2$, $i = 0, 1, \ldots, m$), then Eq. (23) becomes

$$s_i^2 = 4(i+1)^2 \sigma_0^2 \Delta^{2i} \sum_{k=0}^{m} w_k^2 k^{2i}.$$

The sum over k depends only upon the integration scheme and the number of profile points. If we make the further simplifying assumption of equal weights, i.e., that $w_k = m\Delta/m+1$, $k = 0, 1, \ldots, m$—to satisfy the normalization condition

$$\int_0^{q_m} dq = \sum_{k=0}^{m} w_k = q_m —$$

then we have

$$s_i^2 = 4(i+1)^2 \left(\frac{m}{m+1}\right)^2 \Delta^{2i+2} \sum_{k=0}^{m} k^{2i}.$$

The sum over k is now just a polynominal in m of degree $2i+1$. Thus, under these conditions, s_i^2 is roughly proportional to $(i+1)^2 \sigma_0^2 \Delta^{2i+2} m^{2i+1}$ or, equivalently, to $(i+1)^2 \sigma_0^2 p_h^{2i+1} \Delta$. That is, the variance in $\langle p^i \rangle$ increases as the $(2i+1)^{\text{th}}$ power of the momentum range for a fixed spacing of profile points and decreases only linearly with the spacing for fixed range. We therefore expect that for $i = 3$, 4, and possibly 2, lowering the truncation error by increasing p_h may lead to a vastly increased statistical uncertainty in $\langle p^i \rangle$.[19]

The actual situation is somewhat more promising than that outlined above. The assumed condition of equal variance at each profile point is unnecessarily pessimistic. The standard procedure, especially in γ-ray Compton-scattering experiments in which the entire profile is measured at once, is to count for the same period of time at each point. Under these conditions, we have

$$\sigma_j^2 = \sigma_0^2 J_j / J_0 \qquad (j = 0, 1, \ldots, m). \tag{24}$$

The points at high momentum now have lower variances and hence make a smaller contribution to s_i^2. Although an exact expression can no longer be obtained, the dependence on p_h is now closer to p_h^i than to p_h^{2i+1}, as it was in the case of equal σ_j's.

In order to estimate the magnitude of the statistical error to be expected in a typical Compton-scattering experiment, model calculations were carried out for the hydrogen atom, for which

$J(q)$ and $\langle p^i \rangle$ are known exactly. The conditions assumed were (a) equally spaced points separated by 0.1 or 0.01 a.u., and (b) variances of the form (24), with $\sigma_0 = 10^{-2}$, i.e., equal counting times with 10^4 counts accumulated at the peak. The integration was carried out with the trapezoidal rule ($w_0 = w_m = \frac{1}{2}\Delta, w_j = \Delta,\ j = 1, 2, \ldots, m-1$). The results, shown in Table III, are encouraging. The s_i increase relatively slowly with p_h, while a pronounced decrease in standard deviation with decreased point spacing is observed. The values for Δ and p_h used in the calculations are consistent with those employed in most experiments. Also, peak accumulations of 50000 or more counts are frequently reported. There is no doubt that the relatively small increase of s_i with p_h is due in large measure to the rapid falloff of $J(q)$ for the hydrogen atom. We would expect the s_i values for $1s$ electrons of heavier elements to be considerably greater at large p_h. As in the case of truncation error, the $2p$ and other orbitals of principal quantum number greater than 1 give narrower profiles and hence should give smaller contributions than the $1s$ orbital to s_i.

V. CONCLUSIONS

It appears that accurate measurement of $\langle p^{-1} \rangle$, $\langle p^0 \rangle$, and $\langle p \rangle$ is possible for most of the light elements (atomic number less than 10) with present γ-ray techniques. It may also be feasible to measure $\langle p^2 \rangle$ for a few very light elements to an accuracy on the order of 1%. Obtaining reliable values for higher expectation values or more accurate estimates of $\langle p^2 \rangle$ will require improvements in one or more aspects of experimental technique and design.

Since the energy differences between chemical species or between different calculations often amount to only a fraction of 1% of the total energy, it seems worth considering how improved accuracy in $\langle p^2 \rangle$ might be obtained. The problem of truncation error can only be resolved by increasing the range of momenta in the profile. While the present limit of $p = 30$ can probably be increased considerably, it is unlikely that it can be raised by as much as an order of magnitude without a major technological advance. Also, given a fixed number of analyzing channels, increasing p_h must also increase the spacing between points, thereby leading to greater statistical and numerical (integration) errors.

The statistical error may be lowered either by increasing the number of counts taken at each point or by decreasing the spacing between the points. Since the standard deviation in $\langle p^n \rangle$ is proportional to the standard deviation of the individual profile points, halving the standard deviation requires increasing the time of the experiment fourfold. γ rays give much greater Compton-scattered intensity than x rays.[5] A considerable increase in the total number of counts in a given experiment should therefore be feasible. It appears that the γ-ray experiment has not yet been pushed to the limits of instrumental stability, since the aim has been to obtain 1% or better accuracy in $J(q)$ rather than, for example, 10^{-2}% accuracy in $\langle p^2 \rangle$. Nonetheless, it seems unlikely that more than an order of magnitude in accuracy can be gained here. As the results in Table III indicate, there may be much to be gained from taking data at very closely spaced profile points. The limitations here are the channel width and the number of channels available.

Another approach to the problem of statistical error is to take more or more accurate data at high momentum than at low momentum. For example, one might obtain a fixed number of counts at each point instead of counting for a fixed time. In the example $p_h = 15.0$, $\Delta = 0.1$ of Table III, accumulation of 10^4 counts at *all* points leads to a 24-fold decrease in s_2 and a 60-fold decrease in s_4 compared with the values obtained when 10^4

TABLE III. Relative standard deviations $S_i/\langle p^i \rangle$ for the hydrogen atom.[a]

p_h[b]	Δ[b]	0	1	2	3	4
3.0	0.1	4.2×10^{-3}	8.8×10^{-3}	2.1×10^{-2}	3.9×10^{-2}	2.4×10^{-2}
3.0	0.01	1.4×10^{-3}	2.8×10^{-3}	6.8×10^{-3}	8.9×10^{-4}	1.0×10^{-3}
15.0	0.1	4.4×10^{-3}	1.8×10^{-2}	1.7×10^{-1}	3.4×10^{-1}	8.1×10^{-1}
15.0	0.01	1.4×10^{-3}	5.6×10^{-3}	1.8×10^{-2}	1.2×10^{-1}	4.8×10^{0}
30.0	0.1	4.4×10^{-3}	2.1×10^{-2}	3.7×10^{-1}	5.0×10^{-1}	4.8×10^{0}
30.0	0.01	1.4×10^{-3}	6.7×10^{-3}	1.9×10^{-2}	3.7×10^{-2}	4.7×10^{-1}

[a] Calculated from Eqs. (23) and (24) assuming 10^4 counts accumulated at $q = 0$ ($\sigma_0/J_0 = 10^{-2}$).

[b] In a.u.

counts are measured at the peak and all points are counted for the same time. A related approach would be to count all points for a fixed time, but to design the experiment so that the density of points increased with the momentum. Alternatively, one might choose the profile points to give optimal integration accuracy, e.g., as the points for a Gaussian integration scheme.

It seems clear, then, that the best systems to which to apply the methods discussed here are those containing only very light elements. A γ-ray repetition of Eisenberger's[20] x-ray experiments on H_2 and He with more counts, a broader momentum range, and more closely spaced profile points should provide an ideal set of conditions. Other systems of interest might be Li, LiH, and Be (although for these, anisotropy in the profile may be significant), and perhaps the boron hydrides.

Since the main difficulties in calculating expectation values for heavier elements arise from the truncation error in the 1*s* orbital, it should be possible to obtain at least some information about the valence electrons alone. Many Compton-scattering experiments report data for valence electrons only, obtained under the assumption that the core electrons are not affected by chemical bonding, by subtracting profiles calculated from atomic Hartree-Fock wave functions.[21] Currat *et al*.[12] have suggested an approach for experimentally separating the valence and core contributions to the profile. Although such procedures must give rise to additional errors, they may prove useful in providing at least crude estimates of $\langle p^n \rangle$ for heavier elements.

ACKNOWLEDGMENTS

We thank Professor Sidney Golden and Dr. Brian Williams for reading and commenting on the manuscript. Acknowledgment is made to the donors of the Petroleum Research Fund, administered by the American Chemical Society, for support of this research.

APPENDIX

When Slater-type atomic orbitals are employed, the integrals in Eqs. (7) and (8) are all of the form

$$I_n^m(a, b) = \int_0^b p^m/(a^2 + p^2)^n \, dp, \tag{A1}$$

where b may be infinite. The functions I_n^m in Eq. (A1) are directly related to the C and S functions used to compute matrix elements of momentum operators over STOs centered on different atoms.[22]

Differentiating (A1) with respect to a yields the relation

$$I_{n+1}^m(a, b) = -\frac{1}{2na}\frac{d}{da} I_n^m(a, b). \tag{A2}$$

To obtain a recursion relation for the index m, we integrate (A1) by parts to obtain

$$I_n^m(a, b) = \frac{1}{m+1}\left(\frac{p^{m+1}}{(a^2 + p^2)^n}\Bigg|_0^b + 2n\int_0^b \frac{p^{m+2}\,dp}{(a^2 + p^2)^{n+1}}\right) \tag{A3}$$

or, recognizing that the second term on the right-hand side of (A3) is just $2nI_{n+1}^{m+2}(a, b)$, we have

$$I_{n+1}^{m+2}(a, b) = (1/2n)[(m+1)\, I_n^m(a, b) - b^{m+1}/(a^2 + b^2)^n]. \tag{A4}$$

All convergent integrals ($2n - m > 1$) of the form (A1) may be obtained from Eqs. (A2) and (A4) and the integrals

$$I_1^0 = (1/a)\tan^{-1}(b/a),$$

$$I_n^1 = 1/2(1-n)(a^2 + b^2)^{n-1} \qquad (n \geq 2).$$

---

[1]For recent reviews, see (a) M. J. Cooper, Adv. Phys. **20**, 453 (1971); and (b) I. R. Epstein, Accts. Chem. Research **6**, 145 (1973).
[2]M. J. Cooper and J. A. Leake, Philos. Mag. **15**, 1201 (1967).
[3]W. C. Phillips and R. J. Weiss, Phys. Rev. **171**, 790 (1968).
[4]T. Fukamachi, S. Hosoya, Y. Hosokawa, and H. Hirata, Phys. Status Solidi A **10**, 437 (1972).
[5]P. Eisenberger and W. A. Reed, Phys. Rev. A **5**, 2085 (1972).
[6]For a brief review and list of references, see A. C. Wahl and G. Das, Adv. Quantum Chem. **5**, 261 (1970).
[7]For example, (a) R. J. Weiss, J. Chem. Phys. **52**, 2237 (1970); (b) T. Fukamachi and S. Hosoya, J. Phys. Soc. Jap. **28**, 161 (1970).
[8]R. Cheng, B. G. Williams, and M. J. Cooper, Philos. Mag. **23**, 115 (1971).
[9]J. W. M. Dumond, Phys. Rev. **33**, 643 (1929).
[10]G. E. Kilby, Proc. Phys. Soc. Lond. **86**, 1037 (1965).
[11]P. Eisenberger and P. M. Platzman, Phys. Rev. A **2**, 415 (1970).
[12]R. Currat, P. D. Decicco, and R. J. Weiss, Phys. Rev. B **4**, 4256 (1971).
[13]A discussion of the integrals involved in the STO case appears in the Appendix.
[14]The question of momentum expectation values calculated with GTOs has been considered by B. Tsapline [Chem. Phys. Lett. **11**, 75 (1971)].
[15]Although accurate values of a may be obtained by variational calculations, the rules for estimating a given by J. C. Slater [Phys. Rev. **36**, 57 (1930)] provide values of sufficient accuracy for our present purposes.

[16]Note that $\varphi(\underline{G})$ is simply a product of the normal distributions associated with each of the (independent) points in the profile. $\varphi(\underline{G}) = \Pi_{j=0}^{m}[\sigma_j(2\pi)^{1/2}]^{-1} \times \exp[-(J(q_j) - J_j)^2/2\sigma_j^2]$.

[17]W. C. Hamilton, *Statistics in Physical Science* (Ronald, New York, 1964), pp. 149–150.

[18]If one preserves the term $-2p_h^{k+1} j(p_h)$ and uses Eq. (7) rather than Eq. (8) to estimate $\langle p^n \rangle$, the results obtained are $s_i^2 = 4\Sigma_{k=0}^{m} \{q_k^i \sigma_k [(i+1) w_k - \delta_{km}^q]\}^2$. That is, only the mth term in the sum is affected. Since, for example, for $1s$ orbitals $J(p_h) = J(p_0)/(1+s^2)^3$, the difference between Eqs. (7) and (8) is generally small, even for $i = 3$ or 4.

[19]Although this behavior may appear counter intuitive, the explanation lies in the fact that the higher expectation values weight heavily high momentum points for which (under the assumed condition of constant absolute variance) the relative variance is quite large.

[20]P. Eisenberger, Phys. Rev. A **2**, 1678 (1970).

[21]R. J. Weiss, A. Harvey, and W. C. Phillips, Philos. Mag. **17**, 241 (1968).

[22]I. R. Epstein, Chem. Phys. Lett. **9**, 9 (1971).

PHYSICAL REVIEW A VOLUME 8, NUMBER 1 JULY 1973

Electron Spectra from Collisions of O^- and O with Helium*

A. K. Edwards and D. L. Cunningham
Department of Physics and Astronomy, University of Georgia, Athens, Georgia 30602
(Received 15 January 1973)

Three new autodetaching states of O^- have been found and an electron configuration has been assigned one of two previously observed transitions. This gives a total of five known autodetaching states of O^-. Transitions from these states appear as peaks in the spectrum of electrons produced in collisions of O^- ions with a helium target. These peaks lie at 9.50, 10.11, 10.87, 12.12, and 13.71 ± 0.02 eV. The electron spectrum produced by collisions of neutral O with helium shows four autoionizing series of oxygen lying just above the first ionization potential.

INTRODUCTION

The autodetaching states of negative ions have been observed in both electron-scattering experiments[1,2] and in collisional excitation experiments.[3] These states usually take the form of doubly excited configurations which decay by a radiationless transition into a neutral atom and a free electron. The kinetic energy of the free electron is equal to the difference between the excitation energy of the excited ion and that of the remaining neutral atom. In collisional excitation experiments these autodetaching electrons appear as peaks in the energy spectrum of electrons freed by collisions of fast negative ions with target gases.

Collisions of O^- ions with He atoms populate five autodetaching states of O^-. Four are doubly excited states and the other is reached by a $2s \rightarrow 2p$ inner-shell excitation. The four doubly excited states of O^- have been identified theoretically by Matese, Rountree, and Henry (MRH),[4] and our assignment of the inner-shell excitation configuration has been verified by the recent calculations of Chase and Kelly (CK).[5] The good agreement between theory and experiment should remove the unspecified doubts raised by Smith[6] about the acceptableness of the experimental data.

In collisions of H^+ ions with O_2, Rudd and Smith[7] were able to produce several series of autoionizing atomic-oxygen states which lie just above the first ionization potential of oxygen. We have produced these same series by colliding neutral oxygen atoms with helium.

EXPERIMENTAL PROCEDURE

The O^--ion beam is formed in a duoplasmatron ion source[8] using either hydrogen or argon as the discharge gas. The oxygen which forms the negative ions comes, presumably, from the oxide-coated filament of the source. The mass 16 O^- beam is easily separated from the mass 17 OH^- beam by an analyzing magnet placed along the beam path.

The negative ions from the discharge are accelerated (500 eV to 5 keV), momentum-analyzed by deflecting the ions through 45° with a magnet, and focused into a differentially pumped chamber containing a target gas. The target-gas pressure is usually 1–2 m Torr. The beam is collected in a Faraday cup after traversing the collision region and monitored with a beam integrator and microammeter. The method used to record data is shown schematically in Fig. 1.

The electrons leaving the collision region are energy-analyzed using a simple parallel-plate analyzer[9] with a resolution of about 1%, and de-